Supplementary material to: Modelling debris transport within glaciers by advection in a full-Stokes ice flow model.

Anna Wirbel[1], Alexander Helmut Jarosch[2], and Lindsey Nicholson[1]

[1]Institute of Atmospheric and Cryospheric Sciences, University of Innsbruck, Innsbruck, Austria
[2]Institute of Earth Sciences, University of Iceland, Reykjavík, Iceland.

Appendix A: Benchmark tests

A1 Numerical tests following Bochev et al. (2004)

We reproduce the numerical Examples in Bochev et al. (2004). Initial and boundary conditions are initialized in the same manner as described for Example 1 and 2 in Bochev et al. (2004). The computations are perfomed on the unit square ($1\ \mathrm{m} \times 1\ \mathrm{m}$), on an unstructured mesh built out of 874 triangular elements, created with *gmsh* (Geuzaine and Remacle, 2009). The concentration is set up in a continuous piecewise linear function space, resulting in 1821 degrees of freedom. In Fig. A1a, the cell size parameter used for the SUPG (Streamline-Upwind-Petrov-Galerkin) - stabilisation term is shown in colour with the underlying unstructured mesh. In Figs. A1b-c the velocity fields of Example 1 and 2 are illustrated.

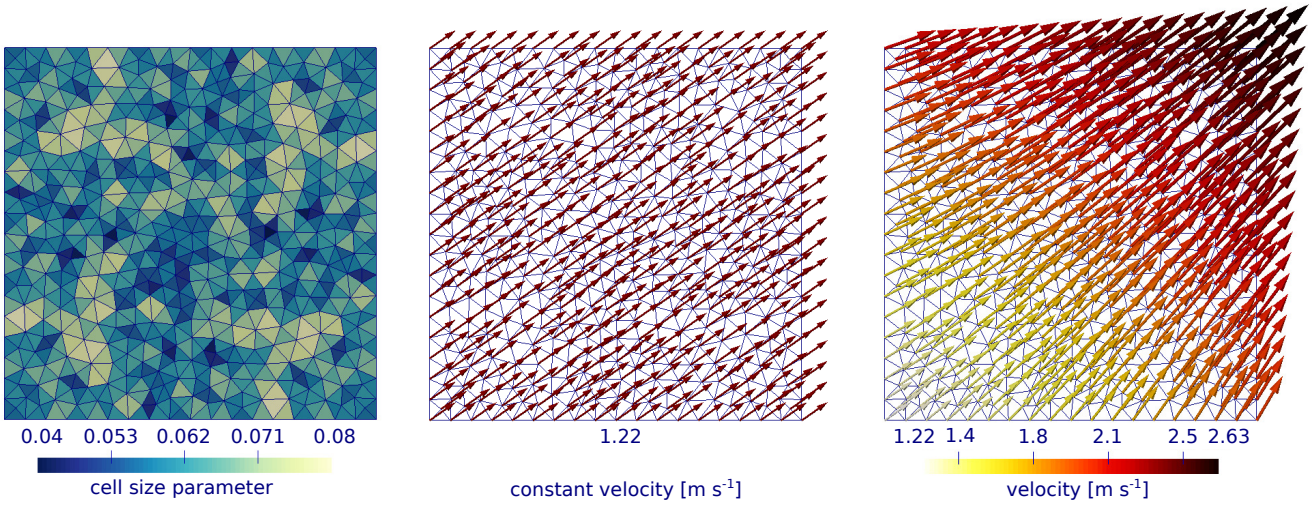

Figure A1. All data is shown for the unit square. (a) mesh cell size parameter, (b) and (c) velocity fields for Examples 1 and 2, arrows represent velocity and are scaled with a factor of 0.07 for clarity.

Following Bochev et al. (2004), the computations are performed for four different time steps: $dt = 0.1$ s, $dt = 0.01$ s, $dt = 0.001$ s, $dt = 0.0005$ s. In Fig. A2, results of Example 1 at total time $t = 0.5$ s, cross-profiles at $y = 0.6$ m and at $x = 0.75$ m, for all four time step settings respectively, are shown. In Fig. A3, results of Example 2 at total time $t = 0.5$ s, cross-profile at $y = 0.85$ m and at $x = 1.0$ m, for all four time step settings respectively, are shown. The results of Example 1 and 2 are in good agreement with the published results in Bochev et al. (2004). The oscillations are stronger, which is mainly caused by the stronger irregularity in mesh cell size in our tests.

Table 1. This table lists the H1 semi-norm for different time steps and Courant-Friedrich-Levy condition parameters, for Examples 1 and 2.

Δt	0.1	0.01	0.001	0.0005
example 1				
$CFL - constant_{mean}$	2.7671	0.2767	0.02767	0.01383
H1 semi-norm	7.3429	4.7117	4.6537	4.65319
example 2				
$CFL - constant_{max}$	4.88407	0.488407	0.0488407	0.0244203
H1 semi-norm	7.5497	3.3116	3.26708	3.26658

A2 Numerical tests following de Frutos et al. (2014)

In this Section, additional figures presenting the results of the "rotating three body problem" (de Frutos et al., 2014) are shown. In Fig. A4a, the respective velocity field is shown. The initial condition, the solution after one full rotation and the over- and undershoots in the solution after one full rotation are illustrated in Fig. A5. In comparison to the refinement time step of 0.1π s presented in the paper, we here employ a refinement time step of 0.01π s. The results demonstrate that the choice of the refinement time step does not affect the quality of the results.

Additionally, we reproduced the three body test with swirling flow conditions (LeVeque, 1996). Because the velocity field of the swirling flow is changing in time, we attached an animation of the evolution of the velocity field for a refinement time step of 0.1π s. In Fig. A6 the results of simulations using a refinement time step of 0.1π s, compared to the refinement time step of 0.01π s used in the paper, are shown.

A3 ISMIP Benchmark test

In order to be able to compare the ice velocities of Haute Glacier d'Arolla computed with *icetools*, to the results of the Ice Sheet Model Intercomparison Project in Pattyn et al. (2008), the computations have been performed using $A = 10^{-16}$ a^{-1}Pa^{-3}. The simulated surface velocitiy is shown in Fig. A7.

A4 2D glacier test cross-sections

In Fig. A8, the location of the cross-sections illustrated in Fig. 11 are indicated.

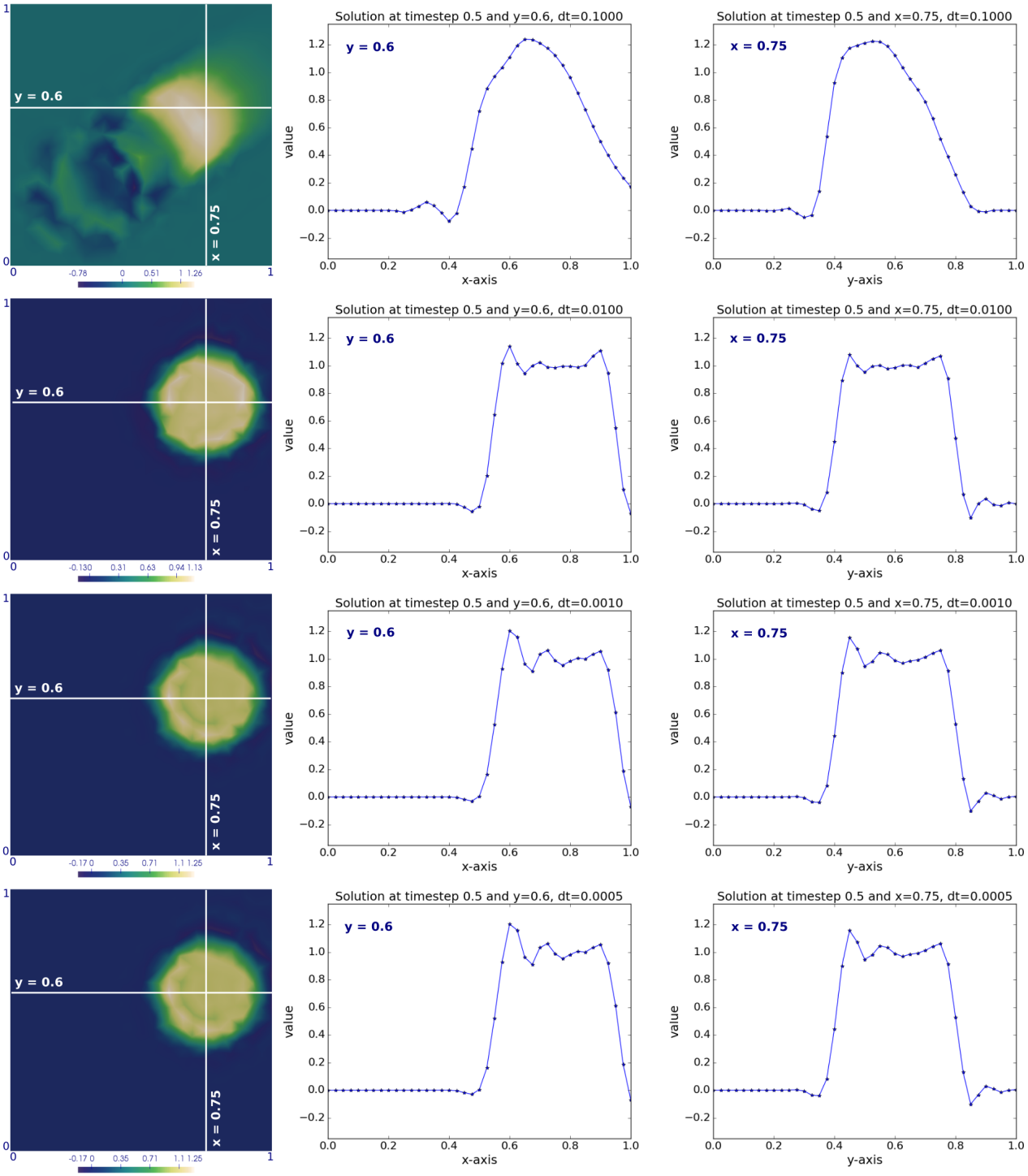

Figure A2. Results of Numerical Example 1. Solutions at $t = 0.5$ s, cross-profiles at $y = 0.6$ m and cross-profiles at $x = 0.75$ m for (top to bottom): $dt = 0.1$ s, $dt = 0.01$ s, $dt = 0.001$ s, $dt = 0.0005$ s.

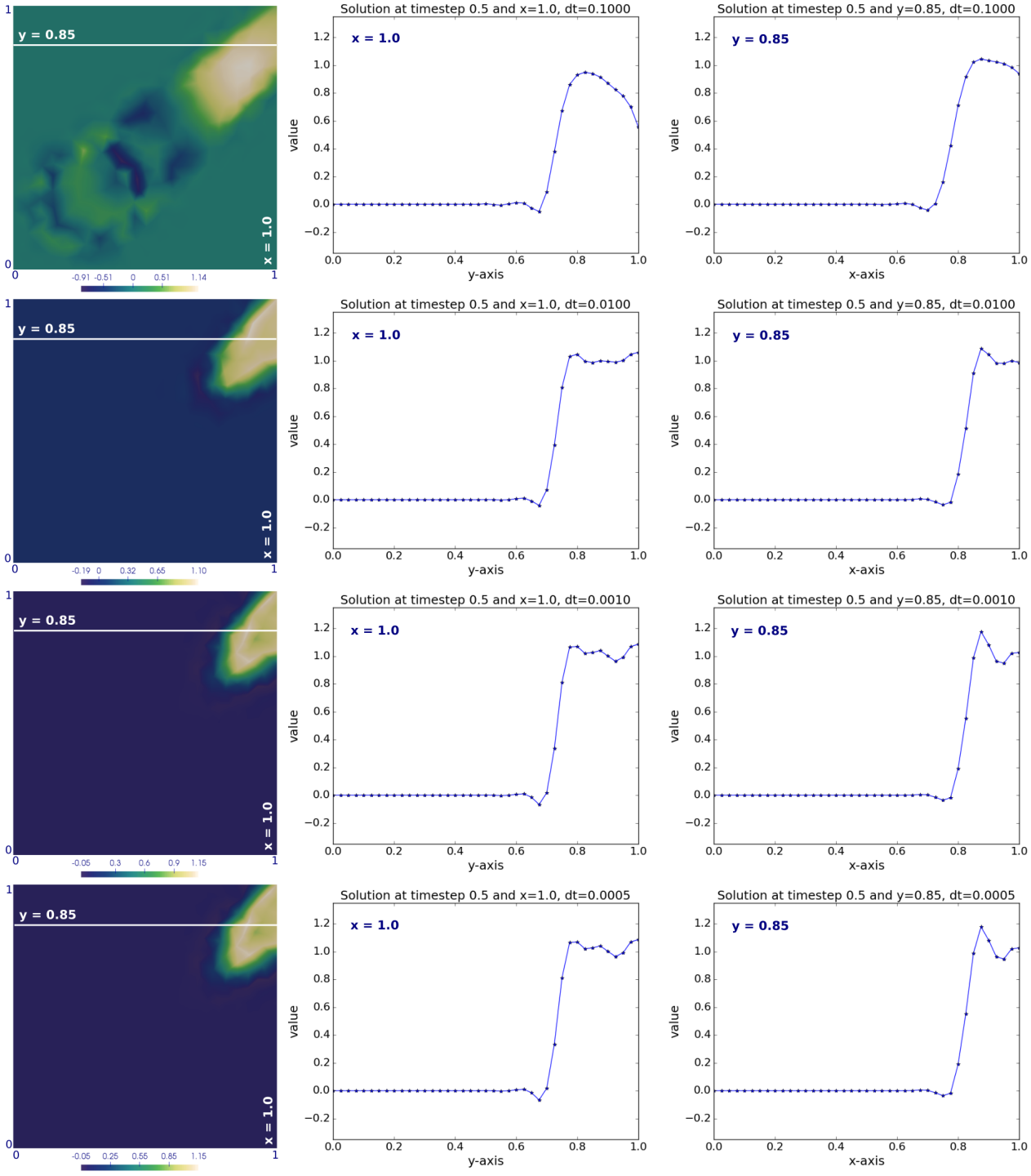

Figure A3. Results of Numerical Example 2. Solutions at $t = 0.5$ s, cross-profiles at $y = 0.85$ m and cross-profiles at $x = 1.0$ m for (top to bottom): $dt = 0.1$ s, $dt = 0.01$ s, $dt = 0.001$ s, $dt = 0.0005$ s.

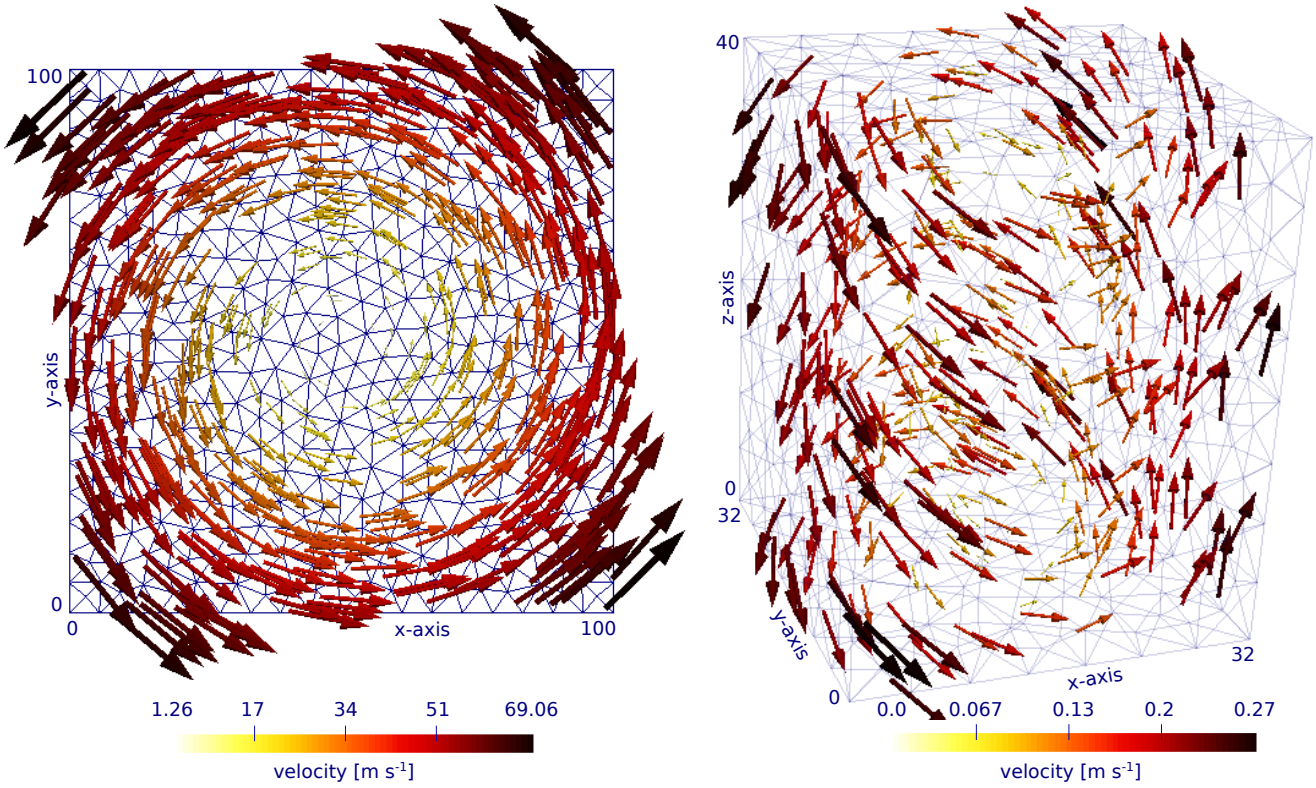

Figure A4. (a) Velocity field of the 2D three body rotation test, arrows represent the velocity and are scaled with a factor of 0.3. (b) Velocity field of the 3D rotation test following (Christensen, 1993), arrows show velocity and are scaled with a factor of 25.

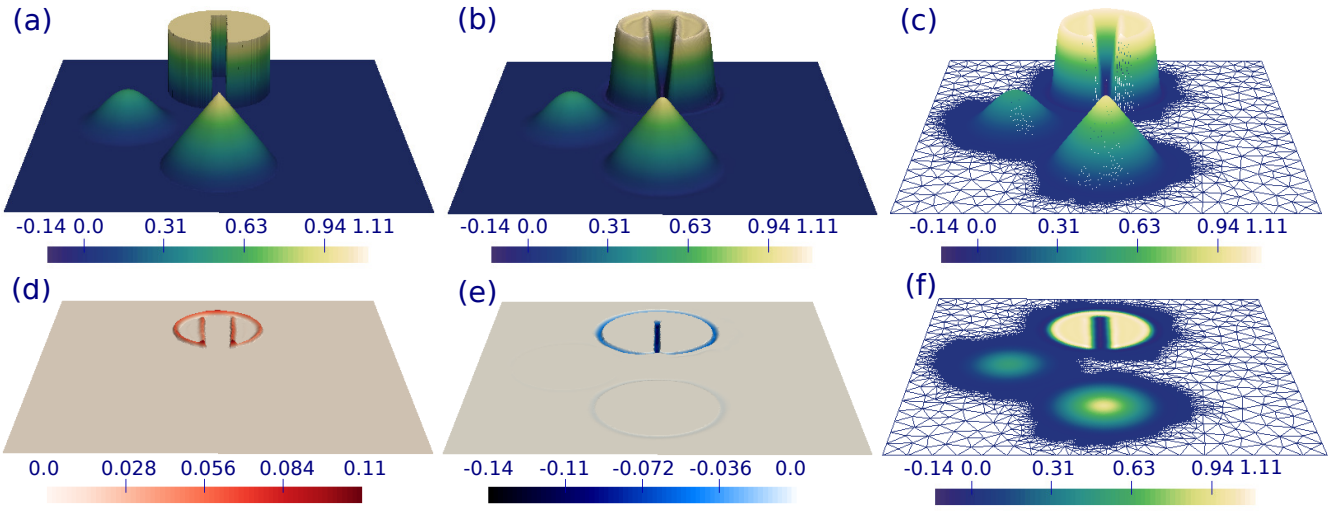

Figure A5. Results of 2D three body rotation test for refinement time step 0.01π s. (a) Initial condition, (b) solution after one full rotation and (c) solution after one full rotation on the underlying mesh. (d) Overshoots (values greater than maximum initial value, as deviation from $max(c_{initial}) = 1.0$) and (e) undershoots (values smaller than minimum initial value, as deviation from $min(c_{initial}) = 0.0$) at t_{total}. (f) Solution after one full rotation on the underlying mesh, shown in plan view. Colour scales show concentration values.

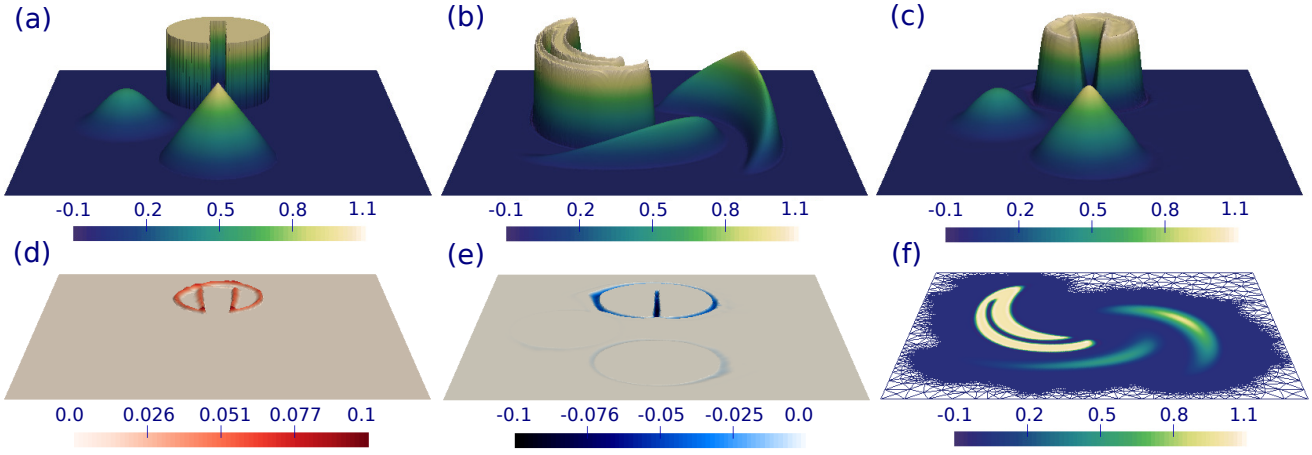

Figure A6. Results of 2D swirling flow three body test for refinement time step 0.1π s. (a) Initial condition, (b) solution at $t_{\text{total}}/2$ and (c) solution at t_{total}. (d) Overshoots (values greater than maximum initial value, as deviation from $max(c_{initial}) = 1.0$), (e) undershoots (values smaller than minimum initial value, as deviation from $min(c_{initial}) = 0.0$) at t_{total} and (f) solution at $t_{\text{total}}/2$ on the underlying mesh, shown in plan view. Colour scales show concentration values.

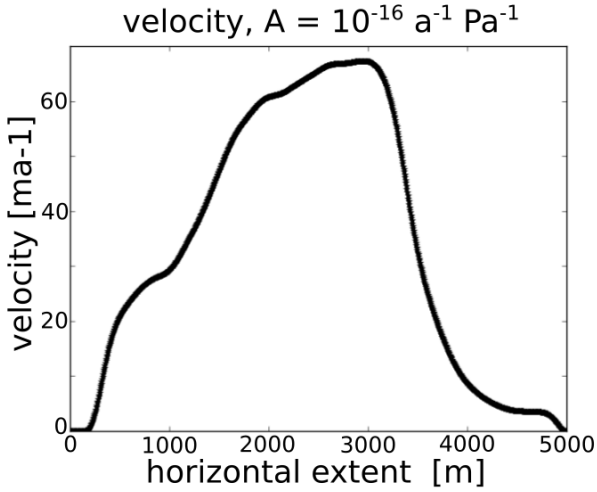

Figure A7. Surface velocity (ma^{-1}) of the longprofile of Haut Glacier d'Arolla computed with $A = 10^{-16}\ \mathrm{a}^{-1}\mathrm{Pa}^{-3}$.

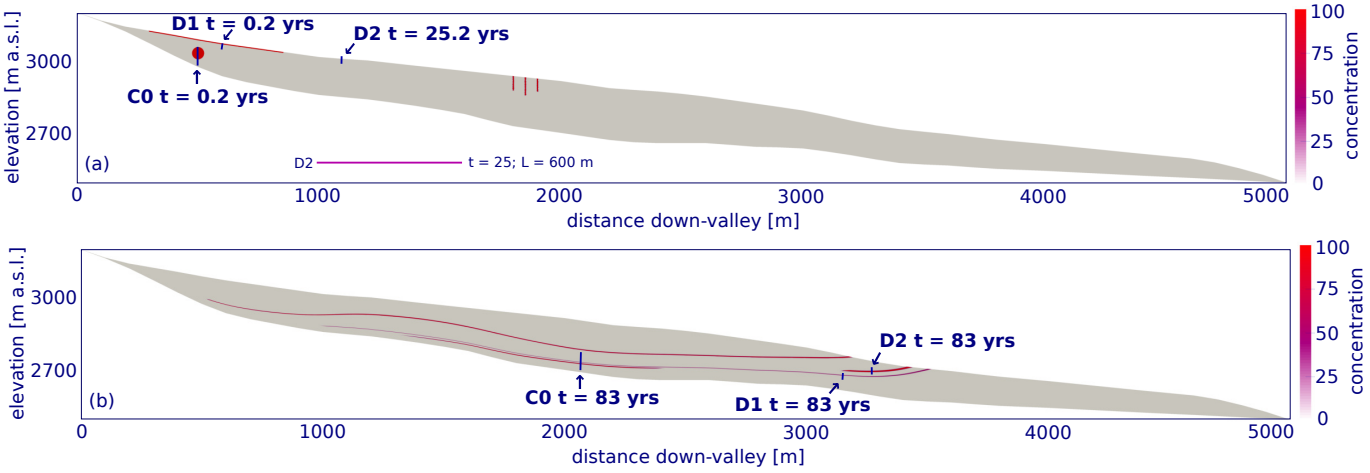

Figure A8. Location of cross-sections of Fig. 11. (a) Time step 0.2 years, blue lines indicate location of starting concentration cross-sections. (b) Time step 83 years, red lines indicate location of end concentration cross-sections.

References

Bochev, P. B., Gunzburger, M. D., and Shadid, J. N.: Stability of the SUPG finite element method for transient advection–diffusion problems, Comput. Method. Appl. M., 193, 2301–2323, doi:10.1016/j.cma.2004.01.026, 2004.

Christensen, J.: Testing Advection Schemes in a Three-Dimensional Air Pollution Model, Math. Comput. Model., 18, 75–88, 1993.

de Frutos, J., García-Archilla, B., John, V., and Novo, J.: An adaptive SUPG method for evolutionary convection–diffusion equations, Comput. Method. Appl. M., 273, 219–237, doi:10.1016/j.cma.2014.01.022, 2014.

Geuzaine, C. and Remacle, J.-F.: Gmsh: a three-dimensional finite element mesh generator with built-in pre-and post-processing facilities, Int. J. Numer. Meth. Eng., 79, 1309–1331, 2009.

LeVeque, R.: High-resolution conservative algorithms for advection in incompressible flow, SIAM J. Numer. A., 33, 627–665, doi:10.1137/0733033, 1996.

Pattyn, F., Perichon, L., Aschwanden, A., Breuer, B., de Smedt, B., Gagliardini, O., Gudmundsson, G. H., Hindmarsh, R. C. A., Hubbard, A., Johnson, J. V., Kleiner, T., Konovalov, Y., Martin, C., Payne, A. J., Pollard, D., Price, S., Rückamp, M., Saito, F., Souček, O., Sugiyama, S., and Zwinger, T.: Benchmark experiments for higher-order and full-Stokes ice sheet models (ISMIP–HOM), The Cryosphere, 2, 95–108, doi:10.5194/tc-2-95-2008, 2008.